

Multifunctional Polymers Based on Ionic Liquid and Rose Bengal Fragments for the Conversion of CO₂ to Carbonates

David Valverde, Raúl Porcar, Pedro Lozano, Eduardo García-Verdugo,* and Santiago V. Luis*

Cite This: *ACS Sustainable Chem. Eng.* 2021, 9, 2309–2318

Read Online

ACCESS |



Metrics & More

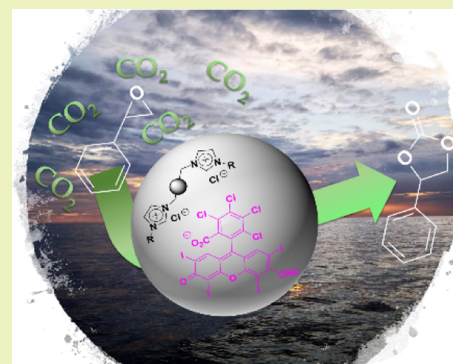


Article Recommendations



Supporting Information

ABSTRACT: Supported ionic liquid-like phases (SILLPs) containing Rose Bengal (RB) units are used to develop organocatalytic systems for the cycloaddition of CO₂ to epoxides. The activity of the supported RB fragments can be fine-tuned by controlling the nature of the SILLPs (i.e., substitution at the imidazolium ring, cross-linking degree of the polymeric matrix, loading, etc.). Such a catalytic system prepared from cheap, simple, and commercially available components provides high activity and stability, with no decay in activity for at least 10 days of continuous use under flow conditions.



KEYWORDS: flow chemistry, supported ionic liquids, CO₂ conversion, catalysis, Rose Bengal

INTRODUCTION

Cyclic carbonates have emerged as compounds of interest for many applications including their use as electrolytes in Li-ion batteries, as polar aprotic solvents for the synthesis of fine chemicals, or as monomers in the preparation of polycarbonates and polyurethanes.^{1–4} Thus, enormous progress has been made in the past few years to improve their synthetic access. In this context, a wide range of catalysts, both homogeneous^{5,6} and heterogeneous,^{7,8} have been developed to carry out their preparation from the CO₂/epoxide ring expansion reaction, through a low carbon footprint process.^{9,10}

Cost-effective CO₂ capture and conversion should increase as much as possible the CO₂ concentration available to the catalysts in the reaction mixture, even at reduced pressure (0.1 MPa). This facilitates achieving more efficient catalytic processes. In this regard, ionic liquids (ILs) can provide a larger CO₂ solubility than other molecular solvents.¹¹ Furthermore, the unique properties of ILs, besides, have been used to fine-tune the catalytic behavior of a variety of catalytic systems including enzymes, organocatalysts, or metal complexes, also for CO₂ conversion.¹² To mitigate some of the limitations for ILs (i.e., ecotoxicity, separation and recovery issues, etc.), supported ionic liquid phases (SILPs) and related polymeric ionic liquids (PILs) have been explored¹³ and some examples of their use for CO₂ transformations have been reported.^{14–17}

The topology and porosity of materials based on supported or polymeric ILs can be also tailored by varying the connectivity, size, and geometry of the building blocks by a bottom-up approach to enhance the control of the reaction.¹³

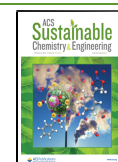
Thus, the design of catalysts supported on materials containing a high density of IL-like fragments and cross-linking degrees (hyper-cross-linked porous materials)¹⁸ may lead to high specific surface areas with a simultaneous enhancement of CO₂ adsorption and catalytic activity. The more efficient concentration of CO₂ and the presence of dual catalytic units may reduce the conditions of temperature and pressure required for its capture and conversion.^{19–21} However, the development of IL-based catalysts able to facilitate the conversion of epoxides at low CO₂ concentrations and pressures (preferably at 0.1 MPa, namely, simple air) remains challenging. The reported catalysts require high CO₂ pressures, usually 5–80 bar, and/or long reaction times to obtain high conversions of cyclic carbonates. Furthermore, despite the heterogeneous nature of these systems, their application under flow conditions is still limited, and in many cases, the systems showed either low activities or significant catalyst leaching.²²

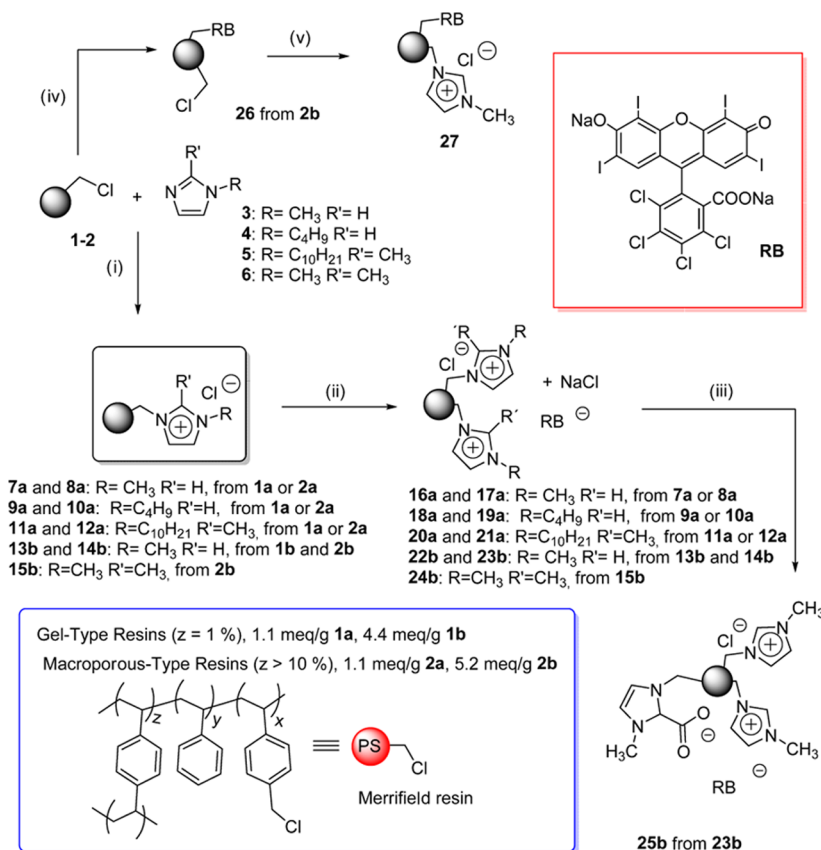
For the first time, this study shows how a simple organocatalyst based on Rose Bengal (RB) immobilized onto supported ionic liquid-like phases (SILLPs) can be used to efficiently transform epoxides into the corresponding cyclic carbonates in the presence of CO₂ with relevant turn over

Received: November 18, 2020

Revised: December 21, 2020

Published: January 19, 2021



Scheme 1. Synthesis of Supported Catalysts^a

^a(i) 80 °C, 150 rpm, 24 h. (ii) RB (C: 1000 ppm), 150 rpm, 12 h, rt. (iii) KHMDs (1.05 equiv), N₂, dry tetrahydrofuran (THF), in the dark, CO₂ balloon, 80 °C, 4 h. (iv) RB: 1–2 (0.15:1 mmol), 60 °C, 150 rpm, 48 h. (v) 60 °C, 150 rpm, 24 h (see Table S1).

number (TON) and turnover frequency (TOF) values. The results demonstrate the presence of a cooperative effect between RB and residual water molecules on the SILLPs, allowing an increase of the activity of the catalytic system. The use of a cross-linked SILLP with the appropriate porosity has allowed the development of a continuous flow system highly active and stable.

RESULTS AND DISCUSSION

Initial Screening. The polymeric supported ionic liquid-like phases (SILLPs) considered in this work were prepared from commercially available Merrifield resins. Initially, both gel-type (**1**) and macroporous (**2**) chloromethylated polystyrene-divinylbenzene (PS-DVB, Scheme 1) resins in the form of beads and with low (1.1 mequiv/g, **1a** and **2a**) or high (4.4 mequiv/g, **1b**; 5.2 mequiv/g, **2b**) chloride loadings were used. The synthetic protocol for the preparation of SILLPs has been already described in detail allowing a quantitative transformation of the chloromethyl fragments into alkyl benzyl imidazolium groups (Scheme 1 and Table S1).^{23,24}

Different PS-DVB materials bearing alkyl imidazolium moieties have been tested as catalysts for the addition of CO₂ to epoxides.^{8,17,25,26} In general, such materials required harsh experimental conditions (temperature >130 °C and pressure >10 bar) to lead to the corresponding carbonates. In this work, styrene oxide (SO) was selected as the epoxide as this is a more demanding substrate, because of its lower reactivity, than other model epoxides commonly used in the literature, allowing a clearer analysis of the different factors

affecting the optimization of the system. Indeed, when the SILLP **7a** was tested as the heterogeneous catalyst for the reaction between SO and CO₂ (see reaction in Scheme 2), only a modest level of conversion (39%) was achieved at 100 °C and 10 bar (Table 1, entry 1).

Two different strategies have been envisioned to enhance the efficiency of these supported ILs. The first one relays on the improvements of the morphological properties of the material, increasing, for instance, the surface area, enhancing

Scheme 2. Cycloaddition Reaction of CO₂ to Styrene Epoxide Catalyzed by Rose Bengal Immobilized onto Supported Ionic Liquid-Like Phases (RB-SILLPs)

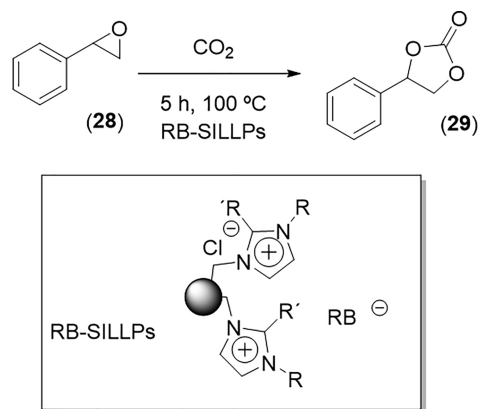


Table 1. Screening of RB-SILLPs as Catalysts in the Reaction between Styrene Oxide (28) and CO₂ to Afford 29^a

7	SILLP	IL loading (mmol/g) ^b	co-catalyst ^c	R	R'	X ⁻	yield ^d	TON ^f
1	7a	1.01		CH ₃	H	Cl	39	78 ⁱ
2	16a	1.01	yes	CH ₃	H	Cl	63	3860
3	16a	1.01	yes	CH ₃	H	Cl	96 ^e	1940
4	22b	3.18	yes	CH ₃	H	Cl	76 ^g	4657
5	18a	0.97	yes	CH ₃ (CH ₂) ₃	H	Cl	31	1899
6	20a	0.88	yes	CH ₃ (CH ₂) ₉	CH ₃	Cl	9	551
7	30a ^h	0.76	yes	CH ₃	H	NTf ₂ ⁻	0	
8				Necker catalyst			0	
9 ^g				PS-DVB unfunctionalized			0	

^aSolventless, 5 h, 100 °C, 10 bar CO₂, 1 mL of epoxide, 36.7 mg of supported cat. gel-type resin. ^bImidazolium unit loading calculated by elemental analysis. ^cRB loading 3.92×10^{-2} μmol RB/g of polymer. ^dCalculated by ¹H NMR. Selectivity >99.9%. ^e111.25 mg of RB-SILLP. ^fTON calculated related to RB loading. ^gMacroporous-type resin. ^hCatalyst prepared from 7a by anion exchange with LiNTf₂. ⁱPolystyrene-divinylbenzene, gel-type resin 2% DVB.

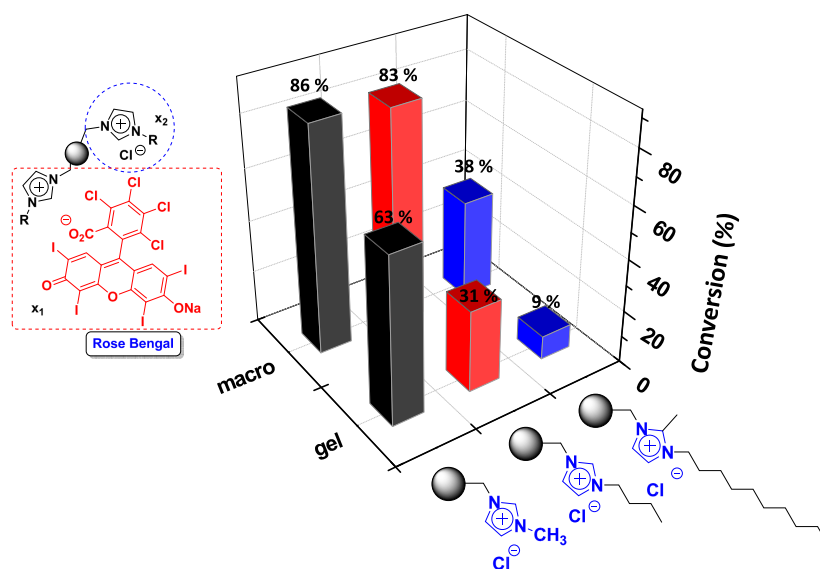


Figure 1. Effect of the support on the efficiency of RB-SILLPs as catalysts in the reaction between styrene oxide (28) and CO₂ to afford 29. ^aConversion determined by ¹H NMR. Selectivity >99.9%.

the accessibility of the functional sites, modifying the cross-linking, etc.^{16,17} The second approach is based on the introduction of additional catalytic moieties (i.e., hydrogen-bond donor (HBD) fragments, metal sites, etc.) to provide acid–base or electrophile–nucleophile double-activation mechanisms, that have been shown to be very efficient in a variety of catalytic systems.^{6–10}

The combination of an organocatalyst with the ionic liquid-like phase of SILLPs was thus considered and Rose Bengal (RB) was initially selected. RB can be easily immobilized onto SILLPs by covalent anchoring (ester formation) or by ionic exchange, just by exposing the corresponding SILLPs to a solution of RB,²⁷ and Zhang, Zhou, and co-workers have exploited rhodamine B (RhB) and rhodamine 6G (Rh6G) in the presence of a base (Et₃N) as organocatalytic systems for the cycloaddition of CO₂ with epoxides.²⁸ RhB and Rh6G are xanthene dyes from the same family of Rose Bengal, which encouraged the study of the cheap and easily prepared polymeric composites RB-SILLPs for this process. In line with those expectations, RB-SILLP 16a containing 3.92×10^{-2} μmol RB/g of polymer provided a conversion of 63% instead of the 39% achieved with the same SILLP in the absence of RB (Table 1, entries 1 vs 2). This represents a TON of 3860 attending to the RB loading. The conversion could be

increased further (up to 96%) doubling the amount of immobilized catalyst used (Table 1, entry 3). It should be mentioned that, under the same experimental conditions, the unfunctionalized PS-DVB polymer was not catalytically active toward cyclocarbonate formation

Encouraged by these results, the effect of different variables was evaluated to optimize the efficiency of the immobilized system. An increase in the amount of the IL-like units in the polymeric RB-SILLPs from 12% (1.01 mequiv/g) to 37% by weight (3.18 mequiv/g) rendered an increase of conversion from 63 to 76% (Table 1, entries 2 vs 4). On the contrary, the exchange of the Cl⁻ counteranion by a less basic and more hydrophobic anion such as NTf₂⁻ led to an inactive system (Table 1, entry 7). It should also be noted that the commercially available RB covalently immobilized onto a PS-DVB support did not provide any catalytic activity under the same experimental conditions (Table 1, entry 8). This result highlights the synergy existing between the RB fragments and the IL-like units of the SILLPs.

Effect of Polymer. The morphology of the polymeric backbone can strongly influence the catalytic activity of polymer-supported systems.²⁹ The initial SILLPs tested were based on gel-type polymers, which are the most classical example PS-DVB resins originally used for solid-phase peptide

synthesis.^{30,31} For those microporous gel-type polymers, the accessibility of the functional sites, and accordingly the reactivity, are dramatically dependent on swelling and, therefore, on the nature of the solvent used. In this regard, it must be noted that the substitution pattern of the imidazolium units induces significant changes in the swelling properties of gel-type SILLPs resins and can be used to tune their catalytic activity.^{16,22,32,33} Although the cycloaddition reaction is performed under solventless conditions, the physicochemical properties of the epoxide (i.e., styrene oxide) will determine the swelling and consequently the accessibility of the catalytic sites on the polymer. When the swelling for these gel-type resins with low loading of IL-like units was measured in styrene oxide (SO), it followed the trend CH_3- (56%) < $\text{CH}_3-(\text{CH}_2)_3-$ (69%) < $\text{CH}_3-(\text{CH}_2)_9-$ (81%). Surprisingly, the swelling did not match the reactivity order. In this case, the use of hydrophobic alkyl residues in the imidazolium fragments produced a significant decay on the activity: CH_3- (63%) > $\text{CH}_3-(\text{CH}_2)_3-$ (31%) > $\text{CH}_3-(\text{CH}_2)_9-$ (9%) (Table 1, entries 2, 5, 6; see also Figure 1), indicating that a more complex mechanism is acting.

To gain additional information on morphology effects, a second family of RB-SILLPs (17a, 19a, and 21a) obtained from the macroporous resin 2a was also assayed for the model reaction. For these resins, displaying a higher cross-linking degree (>10 DVB, 2a), swelling is a less critical parameter as they present a permanent porosity even in the dry state.³⁴ Results obtained with these resins for the cycloaddition reaction between SO and CO_2 at 10 bar are compared with those for their analogous gel-type resins in Figure 1. In both cases, RB supported in SILLPs bearing methylimidazolium units led to the highest conversion independently of the morphology (76% for RB-SILLP 16a gel-type and 85% for the macroporous RB-SILLP 17a). As before, the introduction of hydrophobic chains reduced the activity, although this effect was significantly more important for gel-type resins. Thus, the macroporous resins led to 83 and 38% of conversion for butyl and methyl decyl imidazolium, respectively, while the gel type only achieved 31 and 9% conversions, respectively.

Zhang and co-workers have reported that for homogeneous ILs the conversion of epoxides into cyclic carbonates was faster as the alkyl chain on the imidazolium ring became longer.³⁵ This was related with an increase in the solubility of CO_2 and the epoxide in the IL phase.³⁶ As mentioned above, though changes in swelling for gel-type SILLPs agree well with this, the activity trends observed for both families of SILLPs deviate from the results observed for the homogeneous ILs.

Effect of the Residual Water. In the search for an alternative explanation, the presence of residual water molecules associated with the ionic liquid-like fragments must be considered. ILs are hygroscopic and can absorb significant amounts of water from the atmosphere even when they present hydrophobic structural elements.³⁷ Their hygroscopicity depends on both anion and cation structure, relative humidity, and temperature.³⁸ This is a key factor as the presence of 1 wt % water in an IL can not only enhance their CO_2 absorption capacity from 1:2 to 1:1 mol CO_2/IL ³⁹ but also modify the activity of a given catalyst in homogeneous ILs.^{40,41}

In this regard, the analysis of RB-SILLPs by Fourier transform infrared (FT-IR)-attenuated total reflection (ATR) clearly indicated the presence of residual water, with bands at ca. 3360 and 1613 cm^{-1} . Their intensity was affected by the

substitution of the imidazolium ring and the type of PS-DBV used (Figures S2 and S3), decreasing for hydrophobic alkyl residues in the IL-like units following the trend CH_3- > $\text{CH}_3-(\text{CH}_2)_3-$ > $\text{CH}_3-(\text{CH}_2)_9-$. On the other hand, the intensity was higher for macroporous than for gel-type resins. Finally, the FT-IR-ATR of the resins with a higher loading of IL-like moieties revealed also the presence of a larger amount of residual water (Figure S4).

This residual water content was determined by thermogravimetric analysis (TGA) of the different RB-SILLPs (Table S1).^{42,43} Thus, RB-SILLP 16a ($\text{R} = \text{CH}_3$, $\text{R}' = \text{H}$) showed a water content of ca. 2.01%, while for the most hydrophobic one (RB-SILLP 20a, $\text{R} = \text{CH}_3-(\text{CH}_2)_3$, $\text{R}' = \text{CH}_3$), the water content fell to ca. 1.17%. Noteworthy, macroporous RB-SILLPs revealed a larger water content, ranging from ca. 3.5% for 17a ($\text{R} = \text{CH}_3$, $\text{R}' = \text{H}$) and 2.6% for 19a ($\text{R} = \text{CH}_3-(\text{CH}_2)_3$, $\text{R}' = \text{H}$) to 2.1% for 21a ($\text{R} = \text{CH}_3-(\text{CH}_2)_3$, $\text{R}' = \text{CH}_3$). The loading of IL-like units also affects the amount of residual water. For gel-type resins, this amount changed from 1.81 to ca. 11.35% with the increase of the IL-like loading (RB-SILLPs 16a vs 22b), while for macroporous resins, it changed from 3.46 to 15.14% (RB-SILLPs 17a vs 23b).

Thus, these variations in residual water can be associated with the observed activity changes. It has been demonstrated that the addition of water as a hydrogen-bond donor (HBD) acts as a very efficient co-catalyst for the cycloaddition of CO_2 to epoxides.⁴⁴ Indeed, the right amount of water can lead to a significant increase in activity.⁴⁵ This is clearly observed in the present case when the yields obtained were represented as a function of the molar ratio residual water/epoxide (Figure 2). For both series of RB-SILLPs, gel type and macroporous, yields increase with the water content, and for a given loading and substitution pattern at the imidazolium ring, the yield is always higher for the macroporous polymer displaying a higher residual water content. These findings follow a trend similar to that reported by Zhang and co-workers, who evaluated the effect $\text{H}_2\text{O}/\text{epoxide}$ molar ratio from 0 to 2.⁴⁵ In the low-ratio region (from 0.3 to 0.9), they found how an increase in ratio resulted in a remarkable increase of conversion. Thus, Figure 2a shows how for gel-type resins the conversion increased from 9 to 63% when the water content increases from 0.31 to 0.44. As found by Zhang, yield enhancements are smaller for higher $\text{H}_2\text{O}/\text{epoxide}$ molar ratios. Thus, a change in this ratio from 0.44 to 2.7 (from low to high loading) just provided an enhancement from 63 to 76% (Figure 2b). Macroporous resins, having higher water contents, displayed less pronounced changes. While a reduced number of water molecules can contribute as HBDs to enhance the conversion, higher water contents can reduce activity and selectivity.^{41,42} Reduction in activity has been associated with the strong solvation of the anion that reduces its nucleophilicity, while reduction in selectivity has been ascribed to the formation of diols that starts to be relevant only when excess water is present. Under the conditions considered here, water molecules are not acting as reagents but merely as a component of the catalytic system. This enhancement of the catalytic performance associated with the presence of small amounts of water can be related with the effect of essential water on some natural enzymes used in organic media and in organocatalytic systems.⁴⁶ In some immobilized organocatalysts, the residual water has been observed to play an essential role.^{47,48}

Effect of Pressure. Noteworthy, the reaction could be also performed at atmospheric pressure (CO_2 balloon, Table 2)

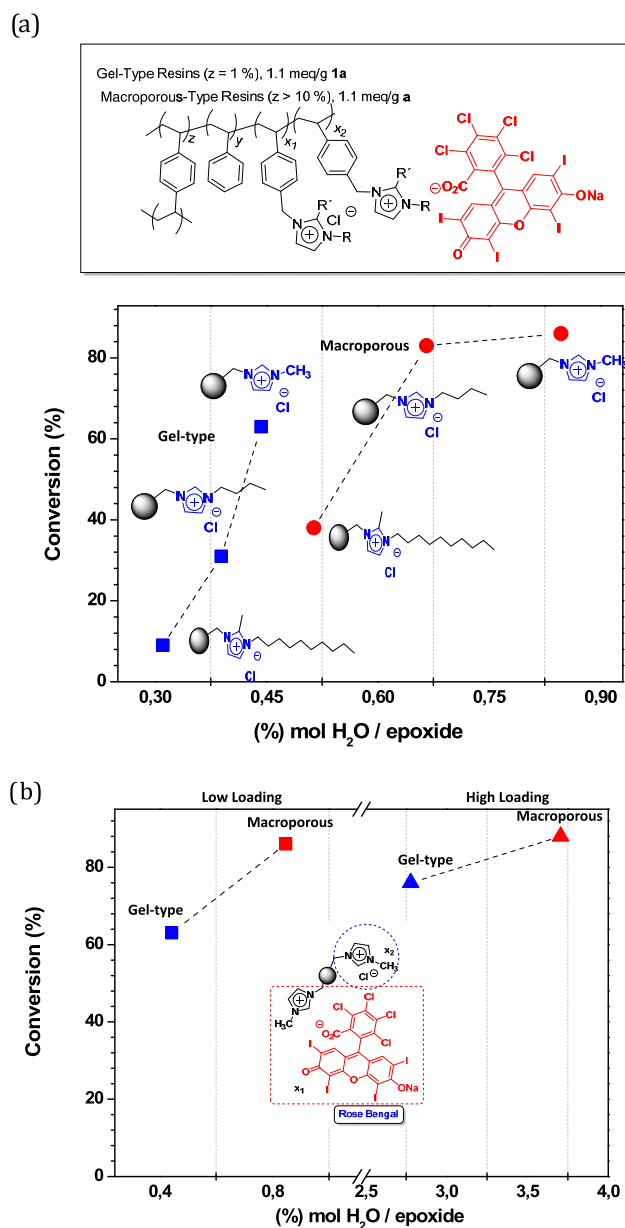


Figure 2. Effect of the residual water on RB-SILLPs in the synthesis of styrene carbonate (29). Conversion vs molar ratio of the residual water in the RB-SILLP with respect to the epoxide. Conversion determined by ^1H NMR. Selectivity >99.9%. Reaction conditions: styrene oxide (1 mL), RB-SILLP (36.7 mg), 10 bar, 100 °C, 5 h. (a) Effect of imidazolium substitution. (b) Effect of the loading.

Table 2. Reaction between Styrene Oxide (28) and CO_2 to Afford 29 at Atmospheric Pressure^a

entry	SILLP	IL loading (mmol/g) ^b	conversion ^c	TON ^e
1	16a	1.2	46	2819
2	16a	1.2	65 ^d	2740
3	17a	1.2	29	1808

^aSolventless, 5 h, 100 °C, CO_2 balloon, 1 mL of epoxide, 36.7 mg of supported catalyst. ^bImidazolium unit loading calculated by elemental analysis. ^cCalculated by ^1H NMR. Selectivity >99%. ^d51.7 mg of RB-SILLP 16a and 14 h. ^eTON calculated related to RB contain.

although, as expected, yields were lower. The gel-type resin RB-SILLP 16a led to a conversion of 46%, which is lower than

the one at 10 bar keeping constant other conditions (entry 1 in Table 2 vs entry 2 in Table 1). The conversion could be increased to the same level achieved at 10 bar by increasing the amount of catalyst by ca. 1.5 and the reaction time from 5 to 14 h (Table 2, entry 2). However, the observed activity trends were reversed at this pressure. Gel-type resins provided better conversions than the analogous macroporous resins: while 46% conversion was obtained for the gel-type resin 16a, the macroporous analogue 17a achieved a 29% conversion (Table 2, entry 1 vs 3). This is likely to be related with the diffusion and concentration of CO_2 achieved under these two conditions (10 bar and atmospheric pressure). Tassaing has shown that in a mixture of CO_2 and SO at 100 °C and 10 bar, the liquid phase is rich in CO_2 . The CO_2 exhibits a significant solubility in SO that increases with pressure at a constant temperature and, therefore, the concentration of CO_2 in the epoxide is reduced at atmospheric pressure.⁴⁹ Under these conditions, CO_2 diffusion can become the limiting factor. Gel-type resins display an excellent swelling in SO that facilitates the accessibility to the catalytic sites presenting reduced diffusional limitations. However, swelling is not relevant in macroporous polymers and the diffusion within the porous structure can be a relevant kinetic factor for low concentrations of CO_2 in SO.

Effect of Catalyst Loading. The use of lower loadings of RB-SILLPs was also investigated (Table 3). Interestingly, the high-loading macroporous catalyst RB-SILLP 23b provided considerable levels of activity even at low loadings.

Table 3. Effect of Catalyst Loading on TOF and TON Values for the Synthesis of Organic Carbonate 29 from SO and CO_2 Catalyzed by RB-SILLP 23b^a

entry	cat. mol % ^b	conversion ^c	TOF ^d	TON ^d
1	0.01632	85	1042	5208
2	0.00328	93	591	28388
3	0.00164	60	509	36634
4	0.00082	68	494	83041

^aSolventless; 5 h; 100 °C; 10 bar CO_2 ; 1, 5, 10, and 20 mL of SO; 36.7 mg of RB-SILLP 23b. ^bMoles of RB with respect to SO. ^cCalculated by ^1H NMR. Selectivity >99%. ^dTOF (h^{-1}) and TON calculated relative to RB loading.

At a loading of 0.016 mol % of RB with respect to SO, a TOF of 1042 h^{-1} per mole of RB was obtained that was reduced to ca. 500 h^{-1} when the loading was further decreased (Table 3, entry 1 vs entries 2–4). The TON, however, was significantly improved at very low loadings, reaching values of up to 83 041 (Table 3, entry 4). This value is in line with those for systems reported in the literature based on a dual activation involving metal catalysts but higher than those for metal-free systems. It must be noted, besides, that the present catalysts are prepared from simple and cheap commercially available resins and modifiers.

Mechanistic Insights. To understand the role played by RB units, we analyzed the catalyst before and after the reaction by FT-IR-ATR. 1,3-Dialkylimidazolium cations paired with basic anions have been found to be good absorbents for CO_2 , since they can react with CO_2 to form zwitterionic NHC- CO_2 adducts.⁵⁰ Both homogeneous and heterogeneous NHC- CO_2 adducts have been used as catalysts for the coupling of CO_2 with epoxides to afford the corresponding carbonates with high efficiency. In RB-SILLPs, RB carboxylate and phenolate groups can enable, in the absence of any additional base, the formation

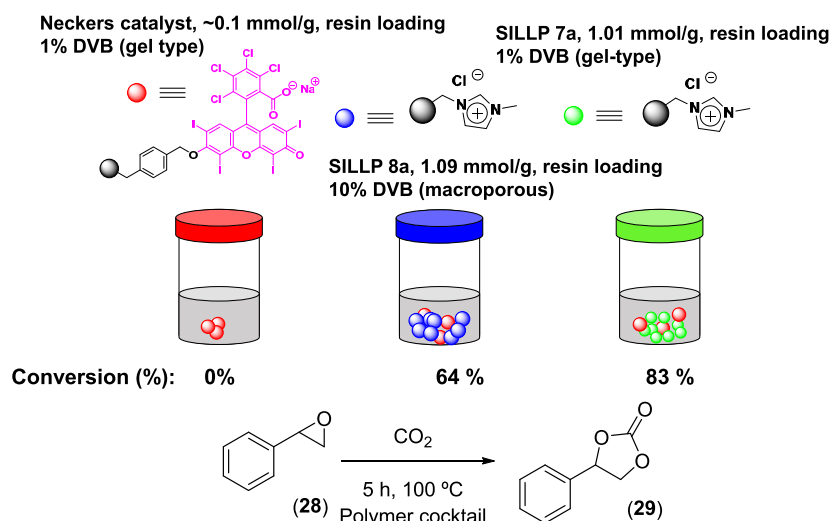


Figure 3. Synergistic effect between of RB and IL-like moieties supported onto polymeric cocktails.

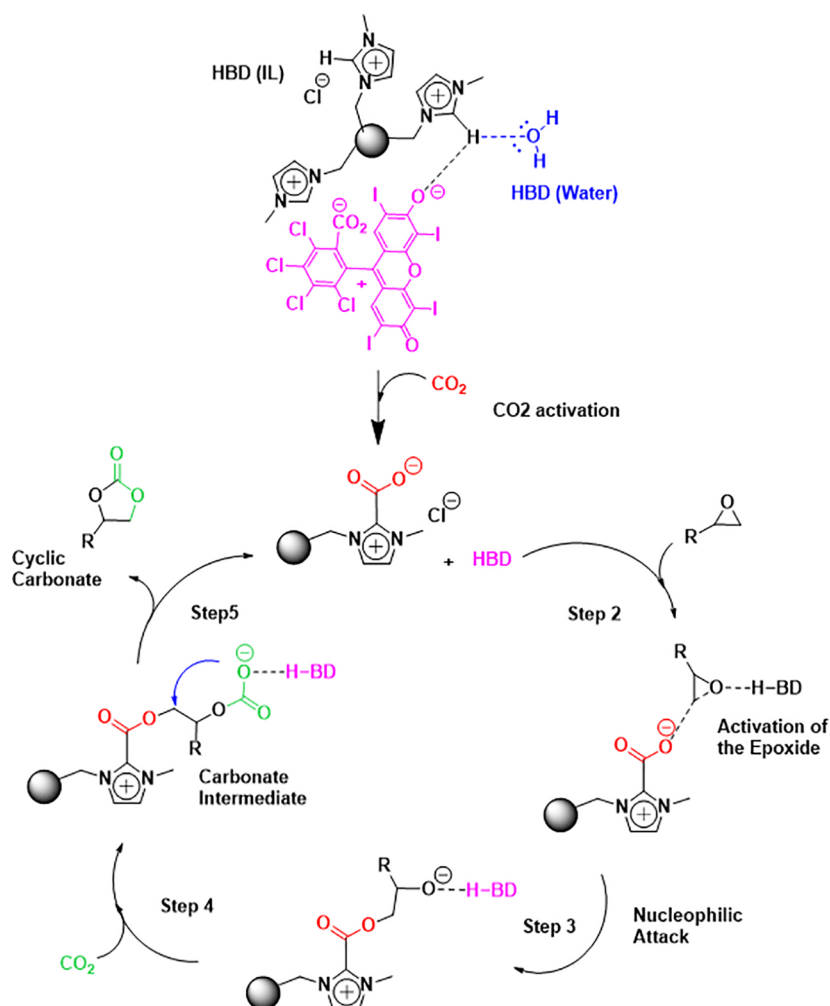


Figure 4. Proposed mechanism for the cycloaddition of CO₂ to epoxides.

of the carbene that in the presence of CO₂ leads to the NHC–CO₂ adduct. The FT-IR-ATR spectrum of RB-SILLP **23b** after the reaction confirmed the formation of this adduct (**25b**, Figure S5). The spectrum showed a band at 1665 cm⁻¹ assignable to the asymmetric $\nu(\text{CO}_2)$ vibrations of N–COO⁻ as well as the disappearance of the bands at 1571

cm⁻¹ for the asymmetric stretching of the CH₂(N)/CH₃(N)–CN, at 1559 cm⁻¹ for $\nu(\text{N}=\text{C})$ and at 1159 cm⁻¹ for C–C stretching and $\delta(\text{CH})$, all of them characteristic of the imidazolium ring (Figure S5). It must be noted that this recovered RB-SILLP was able to act as an efficient catalyst for a new reaction under similar batch conditions.

In view of these results, the preparation of the zwitterionic NHC-CO₂ polymer (31) was assayed following already reported synthetic methods involving deprotonation of the C2 acid proton of the imidazolium in the presence of a base followed by reaction with CO₂.⁵¹ This resin (31) provided the cyclic adduct 29 with a conversion of ca. 80%, slightly lower than the one found for the RB-SILLP 23b (85%). The FT-IR-ATR spectra of this resin before and after reaction showed a band at 1669 cm⁻¹ assignable to the zwitterionic NHC-CO₂ (Figure S6). The spectra for 25b and 31 (Figure S8) are comparable demonstrating the formation of the zwitterionic NHC-CO₂ adduct in the catalytic process. It must be mentioned that SILLP 8a, structurally identical to 17a but lacking RB units, did not show significant changes in the FT-IR spectrum after its use as a catalyst. The lack of the band at 1665–1669 cm⁻¹ (Figure S7) indicates that, in the absence of RB, the NHC-CO₂ adduct was not formed. Altogether, the data suggest that the zwitterionic NHC-CO₂ adduct can be an active species in the catalytic process.

In addition to the use of these multifunctional resins, some polymer cocktails using two different monofunctional resins were also assayed.⁵² In the first one, the macroporous SILLP 8a was mixed with a gel-type resin containing covalently immobilized RB (Neckers catalyst) keeping the same RB/IL-like units molar ratio as in previous experiments. In the second one, two gel-type resins were employed with the use of SILLP 7a. Figure 3 summarizes the results obtained. Remarkably, the Neckers catalyst was not able to catalyze the model reaction. For the polymer cocktails, the one formed involving the macroporous SILLP and the gel-type Neckers catalyst rendered a 64% yield of the carbonate, while the conversion was enhanced for the cocktail formed by the two gel-type resins (83%). Thus, the functionalities present in both the IL-like units and the RB fragments contribute to enhance the reaction of CO₂ and SO. However, the direct interaction between functional groups in two different solid phases is not possible,⁵³ and the involvement of both fragments requires the participation of a species transported between both phases.⁵⁴ Residual water can play the role of facilitating the interaction between RB and IL-like fragments, which is also in agreement with the fact that best results are observed with the cocktail involving two gel-type resins for which the excellent swelling in SO facilitates the transport from one resin to the other.

Figure 4 presents a plausible mechanism in agreement with the experimental data. Imidazolium units can produce NHC fragments with the simultaneous involvement of RB fragments and residual water. Reaction of CO₂ with this NHC forms the zwitterionic NHC-CO₂ (step 1). Both residual water and the imidazolium hydrogen atoms can then act as potential HBD for the activation of the epoxide through hydrogen-bond interactions (step 2). This facilitates the epoxide ring opening by the zwitterionic NHC-CO₂ adduct (step 3). Then, insertion of CO₂ occurs by the nucleophilic attack of the alkoxide formed in the ring opening (step 4), creating a carbonate-ion intermediate, which undergoes intramolecular ring closure, leading to the cyclic carbonate product and restoring the zwitterionic NHC-CO₂ fragment (step 5).

Stability Study. To evaluate the stability of the catalyst, a setup to work under flow conditions represents an optimal system. Thus, a continuous flow reactor, as illustrated in Figure 5, was built formed by two pumps to deliver CO₂ and the epoxide, forming a homogeneous mixture in a mixer and passing through a preheater to reach the reaction temperature

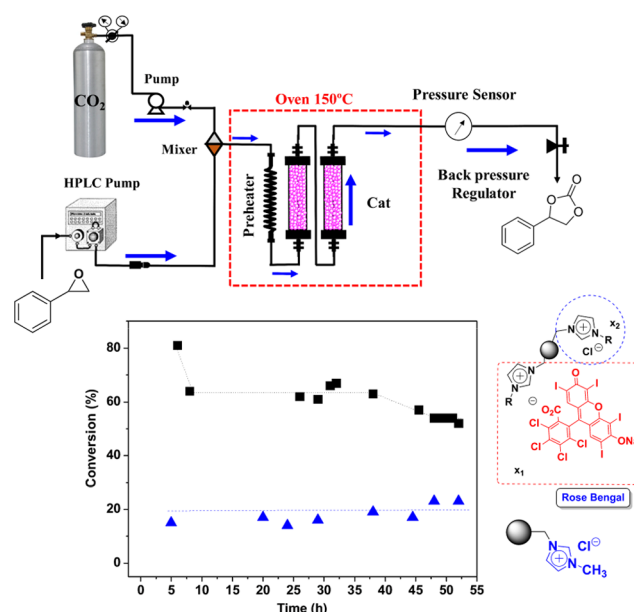


Figure 5. Top: schematic representation of the setup for the continuous flow reactor. Bottom: conversion of SO vs time on stream obtained for the continuous flow reaction between SO and CO₂ at 150 °C and 140 bar. Triangle: 1.892 g of SILLP 14b without RB. Squares: 2.266 g of RB-SILLP 23b. Conversion calculated by ¹H NMR. Selectivity >99%.

before entering in contact with the supported catalyst. Preliminary experiments revealed that CO₂ pressures higher than those for batch experiments were needed, due to the experimental limitations of the continuous setup, to achieve a good access of the two substrates to the catalytic sites for the available residence times. Thus, two reactors in-line packed with the corresponding catalyst were used. Initially, the SILLP 14b, in the absence of RB, was tested at a total flow rate of 55 μL/min, an oven temperature of 150 °C, and a pressure of 140 bar.

This system showed an average conversion of ca. 20% corresponding with a productivity of 0.46 g/(g h). The stability was very good. The catalyst was stable at least during the 55 h tested. The results obtained for the catalyst RB-SILLP 23b bearing RB units confirmed the synergistic effect between RB fragments, water molecules, and IL-like units, providing a more active catalyst and reaching up to 80% conversion for the first few hours of operation. However, after 5 h of continuous use, the activity dropped to ca. 60% conversion. This new level of activity was kept constant till reaching 40 h of operation. After this time, a new drop in activity was again observed (to ca. 50% conversion). This decay in activity can be correlated with the presence of some RB leaching, as the samples at the outlet of the reactor have a slight red coloration. The noncovalent attachment of RB fragments can favor this leaching.

The RB leaching can be avoided using a covalent grafting of both the RB and imidazolium units to the polymeric support. For this, a substoichiometric amount of RB was reacted with the chloromethylated resin to obtain a polymer (26) containing RB units and free -CH₂-Cl groups that were further modified to introduce methylimidazolium moieties (catalyst 27, Scheme 1).⁵⁵ The process could be followed by FT-IR-ATR spectroscopy (Figure S9). In resin 26, the introduction of RB units was confirmed by the appearance of characteristic bands at 1731, 1546, and 1263 cm⁻¹ and the

partial disappearance of the $-\text{CH}_2-\text{Cl}$ band at 1267 cm^{-1} . The introduction of the imidazolium fragments was followed by the complete disappearance of the band at 1267 cm^{-1} and the appearance of bands at 1550 and 1120 cm^{-1} assignable to the imidazolium units. Elemental analysis allowed us to calculate a loading of 1.56 mequiv of RB/g of polymer and 2.23 mequiv of IL-like unit/g of polymer in resin 27.

The reaction between SO and CO_2 was then tested in batch with this new catalyst. After 5 h at $100\text{ }^\circ\text{C}$ and 10 bar, the product 29 was obtained with a conversion of 70%. When catalyst 27 was tested under flow conditions, under the same experimental conditions used for the previous catalysts, the system showed a very stable behavior. An average conversion of 53% was achieved for 10 days of continuous production of the corresponding carbonate (Figure 6).

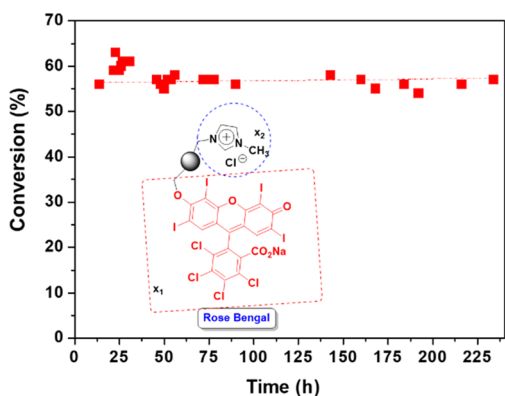


Figure 6. Conversion of SO vs time on stream obtained for the continuous flow reaction between SO and CO_2 at $150\text{ }^\circ\text{C}$ and 140 bar; $50\text{ }\mu\text{L}/\text{min}$ of CO_2 and $5\text{ }\mu\text{L}/\text{min}$ of SO; reactor, 1.906 g of RB-SILLP 27. Conversion calculated by ^1H NMR. Selectivity >99%.

Deactivation after several hours of operation under continuous use is a common trend for immobilized or heterogeneous catalysts.²⁰ In the case of the RB-SILLP 27, no appreciable leaching of RB or decay on the catalytic activity was observed during the 10 days of continuous use. Besides, the productivity of this system was $1.129\text{ g}_{\text{cyclocarbonate}}/(\text{g}_{\text{catalyst}}\text{ h})$, which is among the higher productivities reported so far under continuous flow conditions (Table S2).

CONCLUSIONS

The present results demonstrate that it is possible to develop a sustainable, cheap, and easily accessible multifunctional heterogeneous catalyst using commercially available chloromethylated PS-DVB resin beads modified to introduce IL-like units. The simultaneous presence of RB fragments and residual water molecules that act in combination with supported ionic liquid-like phases produces important synergies, effectively enhancing the catalytic activity of both micro- and macroporous polymer-supported catalysts. Such systems are able to achieve high catalytic activities and excellent selectivities at both atmospheric and 10 bar CO_2 pressures using SO, an epoxide of reduced reactivity, as the substrate. These heterogeneous systems can be systematically optimized considering the loading of the IL-like units, the substitution pattern at the imidazolium rings, and polymer morphology. The resulting organocatalytic optimized supported systems allow reaching TON and TOF values of up to 83 041 and 494 h^{-1} , respectively. Those values are in line with the ones

reported in the literature for systems based on transition metals and involving dual-activation mechanisms. The fact that the catalytic systems presented here are metal-free represents a clear advantage for a green and sustainability approach. Furthermore, these catalysts can be easily prepared and upscaled from simple and cheap commercially available resins and modifiers. Their high stability has been demonstrated using continuous flow systems, although for an efficient access to the catalytic sites, under those conditions. No appreciable loss of activity was observed for at least 10 days of continuous operation, which is a key property in the perspective of a large-scale application. Additional studies are currently being carried out to establish the generality of this approach with the analysis of other related organocatalysts (i.e., simple carboxylates or phenolates).

EXPERIMENTAL SECTION

General Information. All reagents were purchased from Sigma-Aldrich and used without further purification. ^1H and ^{13}C NMR experiments were carried out using a Bruker AVANCE III HD 300 or 400 spectrometer (300 or 400 MHz for ^1H and 125 or 100 MHz for ^{13}C). Chemical shifts are given in δ values, using the residual solvent signal for reference.

Spectroscopic Studies. Fourier transform infrared (FT-IR) spectra were acquired with a Pike single-reflection ATR diamond/ZnSe accessory in a JASCO FT/IR-4700 instrument.

Synthetic Protocols. The synthesis and characterization of SILLPs and RB-SILLPs have been reported in refs 23, 24, and 27.

General Procedure for the Synthesis of Cyclic Carbonate by CO_2 Transformation: Batch Experiments. Two different setups were used for the cyclocarboxylation of SO with CO_2 . The first system, for the reactions under pressure, used a Berghof R-300 high-pressure reactor connected to a pressurized CO_2 source and a back-pressure regulator from Jasco. The heater was first brought to the desired temperature of $100\text{ }^\circ\text{C}$. The reactor was then loaded with styrene oxide (1 mL) and catalyst (35.6 mg). The reactor was connected to the CO_2 pump and the back-pressure regulator and immersed in the bath. CO_2 was liquefied and pumped into the reactor up to the desired pressure, under stirring. After 5 h of reaction, the high-pressure reactor was cooled down and depressurized to atmospheric pressure. Afterward, the reactor was opened and the contents were collected using 1 mL of deuterated chloroform to dissolve the reaction mixture. The catalyst was separated by filtration. ^1H NMR spectra were recorded. Experimental procedures were replicated for all experiments. The average deviation of styrene carbonate formation was less than 5%.

The second one, employed for the reaction at atmospheric pressure, used a round-bottom flask with a CO_2 balloon (100% CO_2) as the gas supply. The same workup as before was used at the end of the reaction.

The signals δ (ppm) for SO are: 2.76 (t, 1H), 3.10 (t, 1H), and 3.82 (t, 1H) for the CH and CH_2 groups and 7.22–7.38 (m, 5H) for the phenyl group. The signals δ (ppm) for the cyclic styrene carbonate are: 4.29 (t, 1H) and 4.82 (t, 1H) for the CH_2 (methylene), 5.70 (t, 1H) for the CH (methine), and 7.22–7.38 (m, 6H) for the phenyl group. No further peaks were detected for all experiments. For all reactions performed, the selectivity was 100%, with no byproducts formation.

Continuous Flow Experiments. SO was pumped using a Jasco HPLC pump at a rate of $5\text{ }\mu\text{L}/\text{min}$. CO_2 was pumped with a refrigerated CO_2 Jasco pump at a flow rate of $50\text{ }\mu\text{L}/\text{min}$. Once CO_2 and epoxide entered in contact in a mixer, they passed through a preheater and two fix-bed reactors charged with the corresponding catalyst. The reactors were located inside an oven to achieve the required experimental temperature. A Jasco back-pressure regulator was connected at the outlet of the second reactor to establish the desired pressure. All required connections were made with a stainless steel 1/16 in. coil. The reaction stream of crude product was collected

in a cold trap at the outlet of the back-pressure regulator. The samples were taken and analyzed by ^1H NMR spectroscopy to determine the conversion and selectivity of the reaction.

■ ASSOCIATED CONTENT

SI Supporting Information

The Supporting Information is available free of charge at <https://pubs.acs.org/doi/10.1021/acssuschemeng.0c08388>.

Structure and properties for the different SILLPs, FT-IR-ATR, and comparison of synthesized SILLPs with some catalysts reported in the literature (PDF)

■ AUTHOR INFORMATION

Corresponding Authors

Eduardo García-Verdugo – Department of Inorganic and Organic Chemistry, Supramolecular and Sustainable Chemistry Group, University Jaume I, E-12071 Castellon, Spain; orcid.org/0000-0001-6867-6240; Email: cepeda@uji.es

Santiago V. Luis – Department of Inorganic and Organic Chemistry, Supramolecular and Sustainable Chemistry Group, University Jaume I, E-12071 Castellon, Spain; orcid.org/0000-0002-8159-3447; Email: luis@uji.es

Authors

David Valverde – Department of Inorganic and Organic Chemistry, Supramolecular and Sustainable Chemistry Group, University Jaume I, E-12071 Castellon, Spain

Raúl Porcar – Department of Inorganic and Organic Chemistry, Supramolecular and Sustainable Chemistry Group, University Jaume I, E-12071 Castellon, Spain; Departamento de Química Orgánica y Bio-Orgánica, Facultad de Ciencias, UNED, E-28040 Madrid, Spain; orcid.org/0000-0002-3345-0804

Pedro Lozano – Dep. Bioquímica y Biología Molecular "B" e Inmunología, Universidad de Murcia, E-30.100 Murcia, Spain; orcid.org/0000-0001-6043-3893

Complete contact information is available at: <https://pubs.acs.org/doi/10.1021/acssuschemeng.0c08388>

Notes

The authors declare no competing financial interest.

■ ACKNOWLEDGMENTS

This work was partially supported by UJI-B2019-40 (Pla de Promoció de la Investigació de la Universitat Jaume I) and RTI2018-098233-B-C22 y C21 (Ministerio de Ciencia, Innovación y Universidades). D.V. thanks UNED (Costa Rica) for the predoctoral fellowship. The authors are grateful to the SCIC of the Universitat Jaume I for technical support.

■ REFERENCES

- (1) Dibenedetto, A.; Angelini, A. Synthesis of Organic Carbonates. In *CO₂ Chemistry*; Aresta, M.; van Eldik, R., Eds.; Advances in Inorganic Chemistry; Academic Press, 2014; Vol. 66, pp 25–81.
- (2) Zhang, X.; Fevre, M.; Jones, G. O.; Waymouth, R. M. Catalysis as an Enabling Science for Sustainable Polymers. *Chem. Rev.* **2018**, *118*, 839–885.
- (3) Yadav, N.; Seidi, F.; Crespy, D.; D'Elia, V. Polymers Based on Cyclic Carbonates as Trait d'Union Between Polymer Chemistry and Sustainable CO₂ Utilization. *ChemSusChem* **2019**, *12*, 724–754.

(4) Dabral, S.; Schaub, T. The Use of Carbon Dioxide (CO₂) as a Building Block in Organic Synthesis from an Industrial Perspective. *Adv. Synth. Catal.* **2019**, *361*, 223–246.

(5) Shaikh, R. R.; Pornpraprom, S.; D'Elia, V. Catalytic Strategies for the Cycloaddition of Pure, Diluted, and Waste CO₂ to Epoxides under Ambient Conditions. *ACS Catal.* **2018**, *8*, 419–450.

(6) Alves, M.; Grignard, B.; Mereau, R.; Jerome, C.; Tassaing, T.; Detrembleur, C. Organocatalyzed Coupling of Carbon Dioxide with Epoxides for the Synthesis of Cyclic Carbonates: Catalyst Design and Mechanistic Studies. *Catal. Sci. Technol.* **2017**, *7*, 2651–2684.

(7) Huang, K.; Zhang, J.-Y.; Liu, F.; Dai, S. Synthesis of Porous Polymeric Catalysts for the Conversion of Carbon Dioxide. *ACS Catal.* **2018**, *8*, 9079–9102.

(8) Marciniak, A. A.; Lamb, K. J.; Ozorio, L. P.; Mota, C. J. A.; North, M. Heterogeneous Catalysts for Cyclic Carbonate Synthesis from Carbon Dioxide and Epoxides. *Curr. Opin. Green Sustainable Chem.* **2020**, *26*, No. 100365.

(9) North, M.; Pasquale, R.; Young, C. Synthesis of Cyclic Carbonates from Epoxides and CO₂. *Green Chem.* **2010**, *12*, 1514–1539.

(10) Kamphuis, A. J.; Picchioni, F.; Pescarmona, P. P. CO₂-Fixation into Cyclic and Polymeric Carbonates: Principles and Applications. *Green Chem.* **2019**, *21*, 406–448.

(11) Chen, Y.; Mu, T. Conversion of CO₂ to Value-Added Products Mediated by Ionic Liquids. *Green Chem.* **2019**, *21*, 2544–2574.

(12) Chaugule, A. A.; Tamboli, A. H.; Kim, H. Ionic Liquid as a Catalyst for Utilization of Carbon Dioxide to Production of Linear and Cyclic Carbonate. *Fuel* **2017**, *200*, 316–332.

(13) Montolio, S.; Altava, B.; García-Verdugo, E.; Luis, S. V. Supported ILs and Materials Based on ILs for the Development of Green Synthetic Processes and Procedures. In *Green Synthetic Processes and Procedures*; Ballini, R., Ed.; Green Chemistry Series; Royal Society of Chemistry: U.K., 2019; pp 289–318.

(14) Valentini, F.; Mahmoudi, H.; Bivona, L.-A.; Piermatti, O.; Bagherzadeh, M.; Fusaro, L.; Aprile, C.; Marrocchi, A.; Vaccaro, L. Polymer-Supported Bis-1,2,4-triazolium Ionic Tag Framework for an Efficient Pd(0) Catalytic System in Biomass Derived γ -Valerolactone. *ACS Sustainable Chem. Eng.* **2019**, *7*, 6939–6946.

(15) Mahmoudi, H.; Valentini, F.; Ferlin, F.; Bivona, L.-A.; Anastasiou, I.; Fusaro, L.; Aprile, C.; Marrocchia, A.; Vaccaro, L. A tailored polymeric cationic tag–anionic Pd(II) complex as a catalyst for the low-leaching Heck–Mizoroki coupling in flow and in biomass-derived GVL. *Green Chem.* **2019**, *21*, 355–360.

(16) Bobbink, F. D.; Dyson, P. J. Synthesis of Carbonates and Related Compounds Incorporating CO₂ Using Ionic Liquid-Type Catalysts: State-of-the-Art and Beyond. *J. Catal.* **2016**, *343*, 52–61.

(17) Luo, R.; Liu, X.; Chen, M.; Liu, B.; Fang, Y. Recent Advances on Imidazolium-Functionalized Organic Cationic Polymers for CO₂ Adsorption and Simultaneous Conversion into Cyclic Carbonates. *ChemSusChem* **2020**, *13*, 3945–3966.

(18) Tan, L.; Tan, B. Hypercrosslinked Porous Polymer Materials: Design, Synthesis, and Applications. *Chem. Soc. Rev.* **2017**, *46*, 3322–3356.

(19) Babu, R.; Kurisingal, J. F.; Chang, J.-S.; Park, D.-W. Bifunctional Pyridinium-Based Ionic-Liquid-Immobilized Diindium Tris(Diphenic Acid) Bis(1,10-Phenanthroline) for CO₂ Fixation. *ChemSusChem* **2018**, *11*, 924–932.

(20) Yue, S.; Wang, P.; Hao, X. Synthesis of Cyclic Carbonate from CO₂ and Epoxide using Bifunctional Imidazolium Ionic Liquid under Mild Conditions. *Fuel* **2019**, *251*, 233–241.

(21) Ziaee, M. A.; Tang, Y.; Zhong, H.; Tian, D.; Wang, R. Urea-Functionalized Imidazolium-Based Ionic Polymer for Chemical Conversion of CO₂ into Organic Carbonates. *ACS Sustainable Chem. Eng.* **2019**, *7*, 2380–2387.

(22) Seo, H.; Nguyen, L. V.; Jamison, T. F. Using Carbon Dioxide as a Building Block in Continuous Flow Synthesis. *Adv. Synth. Catal.* **2019**, *361*, 247–264.

(23) Burguete, M. I.; García-Verdugo, E.; Luis, S. V.; Restrepo, J. A. Preparation of Polymer-Supported Gold Nanoparticles Based on

Resins Containing Ionic Liquid-like Fragments: Easy Control of Size and Stability. *Phys. Chem. Chem. Phys.* **2011**, *13*, 14831–14838.

(24) Burguete, M. I.; Erythropel, H.; Garcia-Verdugo, E.; Luis, S. V.; Sans, V. Base Supported Ionic Liquid-like Phases as Catalysts for the Batch and Continuous-Flow Henry Reaction. *Green Chem.* **2008**, *10*, 401–407.

(25) Xie, Y.; Zhang, Z.; Jiang, T.; He, J.; Han, B.; Wu, T.; Ding, K. CO₂ Cycloaddition Reactions Catalyzed by an Ionic Liquid Grafted onto a Highly Cross-Linked Polymer Matrix. *Angew. Chem., Int. Ed.* **2007**, *46*, 7255–7258.

(26) Wang, T.; Wang, W.; Lyu, Y.; Chen, X.; Li, C.; Zhang, Y.; Song, X.; Ding, Y. Highly Recyclable Polymer Supported Ionic Liquids as Efficient Heterogeneous Catalysts for Batch and Flow Conversion of CO₂ to Cyclic Carbonates. *RSC Adv.* **2017**, *7*, 2836–2841.

(27) Valverde, D.; Porcar, R.; Izquierdo, D.; Burguete, M. I.; Garcia-Verdugo, E.; Luis, S. V. Rose Bengal Immobilized on Supported Ionic-Liquid-like Phases: An Efficient Photocatalyst for Batch and Flow Processes. *ChemSusChem* **2019**, *12*, 3996–4004.

(28) Gong, Q.; Luo, H.; Cao, D.; Zhang, H.; Wang, W.; Zhou, X. Efficient Cycloaddition Reaction of Carbon Dioxide with Epoxide by Rhodamine Based Catalyst Under 1 atm Pressure. *Bull. Korean Chem. Soc.* **2012**, *33*, 1945–1948.

(29) Altava, B.; Burguete, M. I.; Garcia-Verdugo, E.; Luis, S. V. Chiral Catalysts Immobilized on Achiral Polymers: Effect of the Polymer Support on the Performance of the Catalyst. *Chem. Soc. Rev.* **2018**, *47*, 2722–2771.

(30) Seneci, P. *Solid-Phase Synthesis and Combinatorial Technology*, 1st ed.; John Wiley & Sons: New York, 2000.

(31) Dörwald, F. Z. *Organic Synthesis on Solid Phase: Supports, Linkers, Reactions*; Wiley-VCH: Weinheim, 2002.

(32) Zhang, Y.; Zhang, Y.; Chen, B.; Qin, L.; Gao, G. Swelling Poly (Ionic Liquid)s: Heterogeneous Catalysts that are Superior than Homogeneous Catalyst for Ethylene Carbonate Transformation. *ChemistrySelect* **2017**, *2*, 9443–9449.

(33) Zhang, Y.; Wang, B.; Elageed, E. H. M.; Qin, L.; Ni, B.; Liu, X.; Gao, G. Swelling Poly(Ionic Liquid)s: Synthesis and Application as Quasi-Homogeneous Catalysts in the Reaction of Ethylene Carbonate with Aniline. *ACS Macro Lett.* **2016**, *5*, 435–438.

(34) Sherrington, D. C. Preparation, Structure and Morphology of Polymer Supports. *Chem. Commun.* **1998**, *21*, 2275–2286.

(35) Byun, J.; Zhang, K. A. I. Controllable Homogeneity/Heterogeneity Switch of Imidazolium Ionic Liquids for CO₂ Utilization. *ChemCatChem* **2018**, *10*, 4610–4616.

(36) Kawanami, H.; Sasaki, A.; Matsui, K.; Ikushima, Y. A Rapid and Effective Synthesis of Propylene Carbonate Using a Supercritical CO₂-Ionic Liquid System. *Chem. Commun.* **2003**, *7*, 896–897.

(37) Dahi, A.; Fatyeyeva, K.; Chappey, C.; Langevin, D.; Rogalsky, S. P.; Tarasyuk, O. P.; Marais, S. Water Sorption Properties of Room-Temperature Ionic Liquids over the Whole Range of Water Activity and Molecular States of Water in These Media. *RSC Adv.* **2015**, *5*, 76927–76938.

(38) Cammarata, L.; Kazarian, S. G.; Salter, P. A.; Welton, T. Molecular States of Water in Room Temperature Ionic Liquids. *Phys. Chem. Chem. Phys.* **2001**, *3*, 5192–5200.

(39) Zhang, J.; Zhang, S.; Dong, K.; Zhang, Y.; Shen, Y.; Lv, X. Supported Absorption of CO₂ by Tetrabutylphosphonium Amino Acid Ionic Liquids. *Chem. – Eur. J.* **2006**, *12*, 4021–4026.

(40) Yoon, B.; Yen, C. H.; Mekki, S.; Wherland, S.; Wai, C. M. Effect of Water on the Heck Reactions Catalyzed by Recyclable Palladium Chloride in Ionic Liquids Coupled with Supercritical CO₂ Extraction. *Ind. Eng. Chem. Res.* **2006**, *45*, 4433–4435.

(41) Brown, R. A.; Pollet, P.; McKoon, E.; Eckert, C. A.; Liotta, C. L.; Jessop, P. G. Asymmetric Hydrogenation and Catalyst Recycling Using Ionic Liquid and Supercritical Carbon Dioxide. *J. Am. Chem. Soc.* **2001**, *123*, 1254–1255.

(42) Water loss measures the weight loss up to 100 °C after the different SILLPs were left in contact with the air, under the same conditions, for 24 h.

(43) Bobbink, F.-D.; Vasilyev, D.; Hulla, M.; Chamam, S.; Menoud, F.; Laurency, G.; Katsyuba, S.; Dyson, P.-J. Intricacies of Cation–Anion Combinations in Imidazolium Salt-Catalyzed Cycloaddition of CO₂ into Epoxides. *ACS Catal.* **2018**, *8*, 2589–2594.

(44) Alasmay, Y. A.; Pescarmona, P. P. The Role of Water Revisited and Enhanced: A Sustainable Catalytic System for the Conversion of CO₂ into Cyclic Carbonates under Mild Conditions. *ChemSusChem* **2019**, *12*, 3856–3863.

(45) Sun, J.; Ren, J.; Zhang, S.; Cheng, W. Water as an Efficient Medium for the Synthesis of Cyclic Carbonate. *Tetrahedron Lett.* **2009**, *50*, 423–426.

(46) Zaks, A.; Klivanov, A. M. Enzymatic Catalysis in Nonaqueous Solvents. *J. Biol. Chem.* **1988**, *263*, 3194–3201.

(47) Jimeno, C. Water in Asymmetric Organocatalytic Systems: A Global Perspective. *Org. Biomol. Chem.* **2016**, *14*, 6147–6164.

(48) Font, D.; Sayalero, S.; Bastero, A.; Jimeno, C.; Pericàs, M. A. Toward an Artificial Aldolase. *Org. Lett.* **2008**, *10*, 337–340.

(49) Foltran, S.; Cloutet, E.; Cramail, H.; Tassaing, T. In Situ FTIR Investigation of the Solubility and Swelling of Model Epoxides in Supercritical CO₂. *J. Supercrit. Fluids* **2012**, *63*, 52–58.

(50) Wang, Z.; Wang, F.; Xue, X.-S.; Ji, P. Acidity Scale of N-Heterocyclic Carbene Precursors: Can We Predict the Stability of NHC–CO₂ Adducts? *Org. Lett.* **2018**, *20*, 6041–6045.

(51) Zhou, H.; Zhang, W.-Z.; Liu, C.-H.; Qu, J.-P.; Lu, X.-B. CO₂ Adducts of N-Heterocyclic Carbenes: Thermal Stability and Catalytic Activity toward the Coupling of CO₂ with Epoxides. *J. Org. Chem.* **2008**, *73*, 8039–8044.

(52) Sans, V.; Gelat, F.; Karbass, N.; Burguete, M. I.; Garcia-Verdugo, E.; Luis, S. V. Polymer Cocktail: A Multitask Supported Ionic Liquid-Like Species to Facilitate Multiple and Consecutive C-C Coupling Reactions. *Adv. Synth. Catal.* **2010**, *352*, 3013–3021.

(53) Rebek, J.; Gavina, F. Three-Phase Test for Reactive Intermediates. Cyclobutadiene. *J. Am. Chem. Soc.* **1974**, *96*, 7112–7114.

(54) Rebek, J.; Costello, T.; Marshall, L.; Wattlely, R.; Gadwood, R. C.; Onan, K. Allosteric Effects in Organic Chemistry: Binding Cooperativity in a Model for Subunit Interactions. *J. Am. Chem. Soc.* **1985**, *107*, 7481–7487.

(55) Sans, V.; Gelat, F.; Burguete, M. I.; Garcia-Verdugo, E.; Luis, S. V. Polymer-Supported Pd–NHC Complexes: Strategies for the Development of Multifunctional Systems. *Catal. Today.* **2012**, *196*, 137–147.